Mathematical Forum ISSN: 0972-9852
Vol. 31, 2023

Effect of Magneto hydrodynamics hybrid nanofluid flow with thermal radiation and velocity slip parameter

Sewli Chatterjee
Department of Mathematics, THLH Mahavidyalaya (Under Burdwan University), West Bengal 731216, India
Email: sewlichatterjee81@gmail.com

Received on: 24/03/2023
Accepted on: 14/10/2023

Abstract

In this present paper, we studied about the flow behaviour of $ethyleneglycol(EG)$-based Titanium-Dioxide (TiO_2) and Magnesium-Oxide (MgO) hybrid nanofluid passing through a porous surface with the presence of magnetic field. In addition, the convective-heat and slip velocity boundary layer is being considered to generate suction/injection onto the characteristic region. Thermal radiation and heat generation impact also incorporated in the energy equation. A suitable similarity transformation is being used to non – dimensionalize the system of governing equations along with boundary conditions. Final form of equations are solved numerically with the aid of MATLAB software. The converted system of nonlinear ordinary differential equations has been solved numerically by operating Spectral Quasi-linearization method (SQLM). The salient features of convergent flow parameter on velocity and temperature fields are described in the form of graphically. The temperature increases with an enhancement in thermal Biot number for both assisting and opposing flow. It is also found that the heat generation is consequently uplift the thermal boundary layer thickness of hybrid nanofluid flow.

Keywords: Thermal radiation, magneto-hydrodynamics, hybrid nanofluids, Free convection, velocity slip, SQLM.

2010 AMS classification: 47.15.Cb; 44.20.+b;76M25.

1. Introduction

The hybrid nanofluids are the significant features of thermal conductivity and heat transfer effects. In the current study, I have discussed the slip conditions and thermal radiation on a magneto hydro dynamics fluid flow with chemical reaction. The nanofluids are such a fluid in which some nanosized particles like metal or metallic oxide or polymer are combined with some base fluid like as water, oil, and ethylene in such a manner that no sedimentation takes place. This special kind of fluid has a great and considerable industrial and biomedical application in heat and mass transfer, nowadays it has been observed that Hybrid nanofluids are more effective compared to nanofluids in many cases, basically hybrid nano fluids are the combined amalgam of two or more metal, metallic oxide, polymer. This kind of fluids are essentially used for its significant properties in various region like high thermal conductivity, solidity, cooling, heat interchanger. finer heat regulation in electronics devices such as freezer, air-conditioner, generators, power improvement of various motor pumps. Furthermore, economic state to operate hybrid nanofluids are also affordable as it cost low, nowadays its use in various medical experiments, drugs delivery in human bodies is highly considerable, overall effects of hybrid nanofluid are very much remarkable in several wide regions from industrial to medical area.

Typically, thermal radiation is an important parameter in many research it has been found that due to radiation temperature profile increases. Magnetic field has a significant impact in momentum, in presence of it, Lorentz force produces which acts opposite to the velocity, due to this phenomena fluid velocity deteriorates. Many researchers $[1-4]$ examined the behaviour of magnetic field in heat-mass transportation in nanofluid flow. Bagh et al. [5] analysed the Cattaneo–Christov nanofluid model considering microbes and thermal radiation. Brownian diffusion effect with thermophoresis in nanofluid flow has been studied by Ahmad et al. [6]. They noticed that the radial velocity and temperature enhanced with the continuous increment of nanoparticle volume fraction, also found the temperature profile enhanced due to thermal relaxation parameters. Hybrid nanofluid is an amalgam of two or more nanoparticles suspended in suitable base fluid. This kind of fluid has considerable heat and mass transfer capacity compared to ordinary fluid.

In this present paper, hybrid nanofluid is comprising of $ethyleneglycol(EG)$ as base liquid and Titanium Dioxide TiO_2 and Magnesium Oxide MgO as two different metal nanoparticles are used. Choi [7], was the first person who have been studied about the nanofluid in 1995. They found that the nanofluids has a considerable

application in heat exchanger pumping power. Tiwari and Das [8] nanofluid model is a well-known model in this field of nanofluid. Waini et al [9] has been studied about the impact of hybrid nanofluid flow which is a combination of alumina (Al_2O_3) and copper (Cu). They observed that heat transport increases for higher values of radiation parameter with high volume faction of hybrid nanofluid. Kumar KG [10] et.al suggested that heat transfer reduced with the increment of Prandtl number. Shoaib et al. [11] examined about the rotational hybrid nanofluid fluid flow through an extended surface. They numerically investigated the drag coefficient and Nusselt number, also attestor that heat transfer rate enhanced with magnetic parameter. The investigation of Dinarvand et al. [12] is very much considerable in biomedical experiment, they investigated the numerical model of hybrid nanofluid consisting of pure blood as host fluid and TiO_2 and Ag nanosized particles passing through a porous medium, their examination will be a great impact in medical drugs delivery in artery in the human body. Khan et al. [13] tested about SiO_2 & MoS_2 with H_2O hybrid nanofluid. Additionally, Sudarsana Reddy P et al., Waini et al. also investigated the hybrid nanofluid, and indicated the impact of various significant fluid parameters. [14-16].

Shankar et al. [17] did their research on Casson fluid past over a variable permeable medium. They stated if the heat source/sink parameter rises the temperature as well as velocity also enhanced. Anwar et al. [18] used TiO_2 and Ag hybrid nanofluid in blood flow in their experiment, the results are considerable in various medical field. Philip et al. [19] also investigated about blood coagulation in human body. The blood and anticoagulation enhanced the dynamic properties through micro tube. Yaseen [20] have shown about the assisting as well as opposite flow behaviour for different fluid parameters, they also calculated about skin friction, film coefficient coefficient of heat transport and investigated the momentum and energy equation, our paper is an extension of the above paper, we investigated the mass transfer coefficient also in the presence of chemical reactions, which can be very significant in industrial experiments. Moreover, experiments on hybrid nanofluid on numerous conditions has been done by many authors. [21-24]. Waini et al. [25] studied the Buongiorno's model, numerically and also graphically calculated flow behaviour at the equilibrium point.

Careful survey on accessible literature discloses that no peruse have been described to investigate the sequel of chemical reaction, convective heating surface and slip effects on heat transportation and mass characteristics of MHD hybrid nanofluid by considering TiO_2/MgO as different metal nanoparticles and $ethyleneglycol(EG)$ as basic liquid over permeable moving surface. The converted differential equations

have been decoded using SQLM technique. The problem inscribed in this inspection has instantaneous applications for cooling purpose in electronic, transformer, generator etc.

2. Mathematical Formulation

Consider steady, two – dimensional, convective and MHD boundary layer heat and mass transfer of $TiO_2/MgO - ethyleneglycol(EG)$ based hybrid nanofluid flow past a permeable moving surface with slip effects. To inspect the heat and mass transfer ability of hybrid nanofluid flow through a porous medium, heat source/sink, thermal radiation, velocity slip, Suction/injection and chemical reaction effects has been considered. This article exhibits the contrast of hybrid nanofluid flow posture considering buoyancy flow. Fig. 1 demonstrate the geometry of the ongoing investigation. The $x - axis$ is measured in the direction of flow and parallel to the lamina, while the $y - axis$ is measured normally to the lamina.

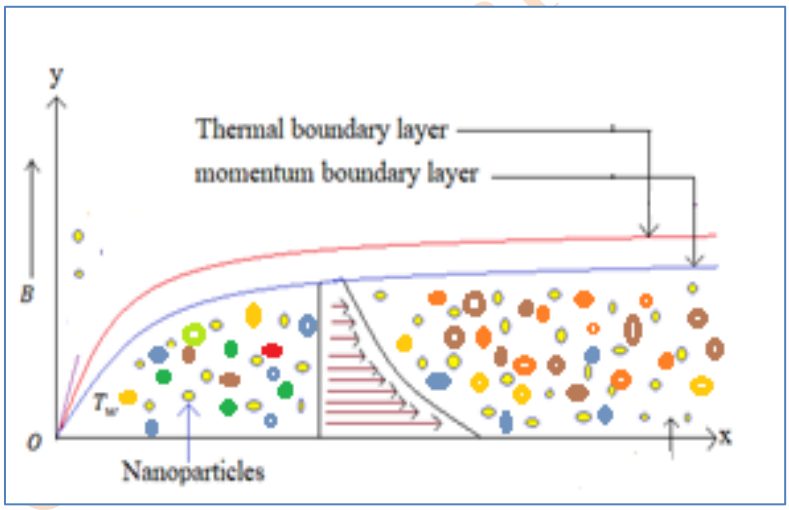

Fig. 1: Coordinates system of the flow model

Magnetic field of strength $B = \frac{B_0}{\sqrt{2x}}$ has been applied normally to the sheet. $v_w(x)$ denotes mass flux velocity. $v_w(x) < 0$ stand for suction whereas $v_w(x) > 0$ prevail injection. Q_0^*, h_f^*, h_c^*, k'^* and β^* are functions of x only which denotes the heat source, convective heat transfer coefficient,

Under prior conventions, boundary layer leading equations of the stream associated with hybrid nanofluid along with convection and slip effects, porous media, thermal radiation $(Rd)$are given by :

Continuity equation:

$$\frac{\partial u}{\partial x}+\frac{\partial v}{\partial y}=0 \tag{1}$$

Momentum equation:

$$u\frac{\partial u}{\partial x}+v\frac{\partial u}{\partial y}=\frac{\mu_{hnf}}{\rho_{hnf}}\frac{\partial^2 u}{\partial y^2}+\frac{\sigma_{hnf}B^2}{\rho_{hnf}}(u_\infty-u)+\frac{(\rho\beta^*)_{hnf}\,g}{\rho_{hnf}}(T-T_\infty)-\frac{\nu_{hnf}}{K^*}u \tag{2}$$

Energy equation:

$$u\frac{\partial T}{\partial x}+v\frac{\partial T}{\partial y}=\frac{k_{hnf}}{(\rho c_p)_{hnf}}\frac{\partial^2 T}{\partial y^2}-\frac{1}{(\rho c_p)_{hnf}}\frac{\partial(q_r)}{\partial y}+\frac{Q_0^*}{(\rho c_p)_{hnf}}(T-T_\infty) \tag{3}$$

Boundary conditions:

The relevant boundary conditions are:

$$u=U\alpha+k'^*\frac{\partial u}{\partial y},\ v=v_w(x),\ -k_{hnf}\frac{\partial T}{\partial y}=h_f^*(T_w-T), y=0$$

$$u=u_\infty\to U,\quad T\to T_\infty,\ \text{as } y\to\infty \tag{4}$$

Here $(x,\ y)$ are cartesian coordinates, $[u,v]$, T, μ_{hnf}, ν_{hnf}, κ_{hnf}, ρ_{hnf}, $(\rho C_p)_{hnf}$, σ_{hnf}, and β_{hnf} are velocity vector, temperature of the hybrid nanofluid, dynamic viscosity, kinematic viscosity, thermal conductivity, density, specific – heat capacitance, electrical conductivity, thermal expansion coefficient of the hybrid nanofluid, orderly. In addition, g is the acceleration due to gravity, k'^* denotes slip length, K^* stands for porous medium permeability, R_1 signifies chemical reaction rate, q_r stands for the radiative heat flux, Q_0^* signifies the coefficient of heat source/sink. In the present paper, hnf signifies $TiO_2-MgO/ethylene\ glycol$ hybrid nanofluid, nf signifies the nanofluid and f stands for base fluid.

$\alpha>0$ $(positive\ moving\ parameter)$ characterize downstream movement of the surface from the origin, whereas $\alpha<0$ $(negative\ moving\ parameter)$ indicates upstream movement of the lamina from the origin.

The approximate Rosseland form is utilized in energy equation (2) to integrate radiative consequence and is defined as:

$$q_r = -\left(\frac{4\sigma^*}{3k^*_{hnf}}\right)\left(\frac{\partial T^4}{\partial y}\right) \tag{5}$$

Here σ^* indicates Stefan – Boltzmann constant and k^*_{hnf} signifies coefficient of mean absorption.

Presuming the temperature difference (ΔT) to be insignificant in the stream, we have :

$$T^4 \cong 4T_\infty^3 T - 3T_\infty^4 \tag{6}$$

Utilizing (5) and (6), we reconsider (3) as:

$$u\frac{\partial T}{\partial x} + v\frac{\partial T}{\partial y} = \frac{k_{hnf}}{(\rho c_p)_{hnf}}\frac{\partial^2 T}{\partial y^2} + \frac{1}{(\rho c_p)_{hnf}}\left(\frac{16\sigma^* T_\infty^3}{3k^*_{hnf}}\right)\left(\frac{\partial^2 T}{\partial y^2}\right) + \frac{Q_0^*}{(\rho c_p)_{hnf}}(T - T_\infty) \tag{7}$$

The following applicable Similarity transformations are proposed as to convert the leading PDEs to ODEs:

$$u = Uf'(\eta),\ v = \sqrt{\frac{U\nu_f}{2x}}\big(\eta f'(\eta) - f(\eta)\big),\ \theta(\eta) = \frac{T - T_\infty}{T_w - T_\infty},\ \eta = y\sqrt{\frac{U}{2x\nu_f}} \tag{8}$$

And the mass flux velocity is presented as:

$$v_w(x) = -\sqrt{\frac{U\nu_f}{2x}}S \tag{9}$$

The Eqs. (2) and (3) are converted into the following forms orderly as shown below:

$$ff'' + \frac{1}{AB}f''' + \frac{C}{B}M(1 - f') + 2D\lambda\theta - \frac{1}{AB}K_p f' = 0 \tag{10}$$

$$\left(\frac{k_{hnf}}{k_f} + \frac{4}{3}R_d\right)\theta'' + E\,Pr\,f\theta' + 2Pr\,Q\,\theta = 0 \tag{11}$$

And the boundary conditions (4) converted as follows:

$$f(\eta) = S,\ f'(\eta) = \alpha + \gamma f''(\eta),\ -\frac{k_{hnf}}{k_f}\theta'(\eta) = Bi_t\big(1 - \theta(\eta)\big),$$

$$f'(\eta) = 1,\ \theta(\eta) = 0, \text{ at } \eta = 0 \tag{12}$$

The associated dimensionless parameters are interpreted as			
Parameter	Name	Expression	
$\boldsymbol{M}$	Magnetic parameter	$M = \frac{\sigma_f B_0^2}{\rho_f U}$	
$\boldsymbol{K_p}$	Porosity parameter	$K_p = \frac{\nu_f (2x)}{K^* U}$	
$\boldsymbol{Rd}$	Thermal radiation parameter	$Rd = \frac{4\sigma^* T_\infty^3}{k_{hnf}^* k_f}$	
$\boldsymbol{\lambda}$	Mixed convection parameter	$\lambda = \frac{Gr_x}{Re_x^2} = \frac{g\beta_f (T_w - T_\infty)}{U^2}$	$\lambda = 1$ $(Assisting\ flow)$ $\lambda = -1$ $(Opposing\ flow)$
$\boldsymbol{Pr}$	Prandtl number	$Pr = \frac{\mu_f (c_p)_f}{k_f}$	
$\boldsymbol{Q}$	Heat source/sink parameter	$Q = \frac{Q_0}{U(\rho c_p)_f}$	
$\boldsymbol{S}$	Constant mass flux parameter	$S > 0$ $(fluid\ suction)$ $S < 0$ $(fluid\ injection)$	
$\boldsymbol{\gamma}$	Velocity slip parameter	$\gamma = k' \sqrt{\frac{U}{2\nu_f}}$	
$\boldsymbol{B_{i_t}}$	Thermal Biot number	$B_{i_t} = \frac{h_f}{\kappa_f} \sqrt{\frac{2\nu_f}{U}}$	
$\boldsymbol{A}$	–	$A = \frac{\mu_f}{\mu_{hnf}}$	–
$\boldsymbol{B}$	–	$B = \frac{\rho_{hnf}}{\rho_f}$	–
$\boldsymbol{C}$	–	$C = \frac{\sigma_{hnf}}{\sigma_f}$	–
$\boldsymbol{D}$	–	$D = \frac{\beta_{hnf}}{\beta_f}$	–
$\boldsymbol{E}$	–	$E = \frac{(\rho C_p)_{hnf}}{(\rho C_p)_f}$	–

$\lambda > 0$ symbolize aiding flow and opposing flow is indicated by $\lambda < 0$.

1.1. Drag force and Nusselt number

Potential amounts of awareness in this perusal of heat transfer, which controlled the inflow are the drag force (C_f) and the local Nusselt number (Nu_x) which are defined as:

$$C_f = \frac{\tau_w}{\rho_f U^2},\ Nu_x = \frac{x(q_w+q_r)}{\kappa_f(T_w-T_\infty)} \tag{13}$$

Sum of $q_w\ (heat\ flux\ on\ the\ lamina)$ and $q_r\ (radiative\ heat\ flux)$ i.e., $(q_w + q_r)$, wall shear stress τ_w are given as:

$$q_w + q_r = -\left(\kappa_{hnf}\frac{\partial T}{\partial y} + \frac{4\sigma^*}{3k^*_{hnf}}\frac{\partial T^4}{\partial y}\right)\Big|_{y=0},\ \tau_w = \mu_{hnf}\left(\frac{\partial u}{\partial y}\right)\Big|_{y=0} \tag{14}$$

Implementing the dimensionless transformations (13) and Eq. (14), we acquire

$$\sqrt{Re_x}C_f = \frac{1}{\sqrt{2}A}f''(0),\ \frac{Nu_x}{\sqrt{Re_x}} = -\frac{1}{\sqrt{2}}\left(\frac{\kappa_{hnf}}{\kappa_f} + \frac{4}{3}R_d\right)\theta'(0) \tag{15}$$

where $Re_x = \frac{Ux}{\nu_f}$ is the local Reynolds number.

Table 1 illustrates the quantifiable aspects of thermophysical parameters of $ethylene\ glycol$ and $(TiO_2 - MgO)$ metal nanoparticle are given below [20].

Table 1 – Thermal characteristics of base – fluid and nanosolid particles

Thermophysical	$\rho(Kg/m^3)$	$C_p(J/KgK)$	$\kappa(W/mK)$	$\beta(1/K)$	$\sigma(\Omega m)^{-1}$
ethylene glycol (EG)	1110	2400	0.253	65	5.5×10^{-6}
Titanium Dioxide (TiO_2)	4250	686.2	8.9538	0.9	2.38×10^{6}
Magnesium oxide (MgO)	3560	955	45	1.26	1.42×10^{-3}

2. Result and discussions

In this column, we demonstrate the impact of several parameters as thermal Biot number (B_{i_t}), porosity parameter (K_p), suction/injection parameter (S), local mixed convection (λ), moving parameter (α), heat source/sink parameter (Q), Radiation parameter (R_d), magnetic field parameter (M), velocity slip parameter (γ) on $TiO_2 - MgO/EG$ hybrid nanofluid flow and thermal boundary layer in the current model. In this column, $\lambda = -1$ signifies contending flow and $\lambda = 1$ indicates aiding flow.

Furthermore, throughout the discussion, it has been considered that the values of each parameter are constant.

Fig. $2(a)$ highlights the impact of thermal Biot number (B_{i_t}) on the velocity layout $f'(\eta)$. We have demonstrated the repercussion of B_{i_t} for both aiding flow $(\lambda = 1)$ and contending flow $(\lambda = -1)$ cases. For $\lambda = 1$ (aiding flow), the velocity increase together with an enhancement in thermal Biot number (B_{i_t}) while for contending flow a contrary result has been observed.

Fig. $2(b)$ sketched the repercussion of B_{i_t} on $\theta(\eta)$. Thermal Biot number is associated with convective heat transfer coefficient (h_f). The numerical enhancement in B_{i_t} associated with convective heating at the wall. Additionally, hike in thermal Biot number (B_{i_t}) generate a significant temperature difference (ΔT) at the surface $(\eta = 0)$. Moreover, an increment in the thermal layout has been observed with rising thermal Biot number. When the thermal Biot number increases, there is a notable reduction in the thermal resistance of the surface. We witness noteworthy upsurge in thermal boundary layer thickness because of the increase in convection. The temperature increases with an enhancement in thermal Biot number for both assisting and opposing flow.

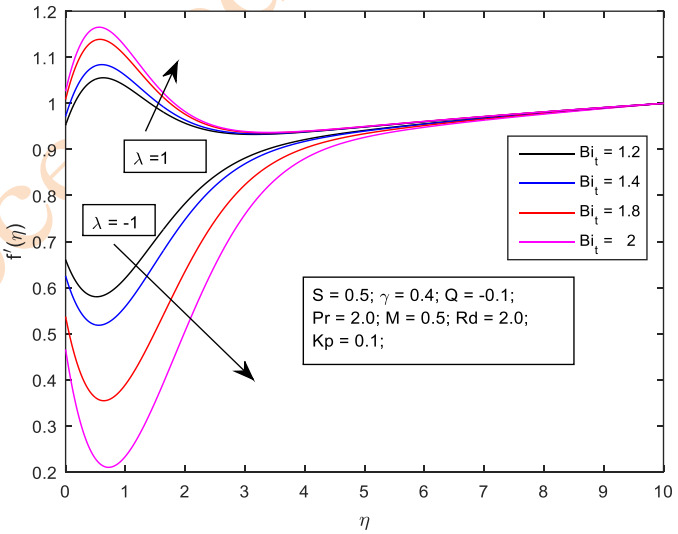

Fig.2(a): Impact of thermal Biot number B_{i_t} on velocity layout $f'(\eta)$.

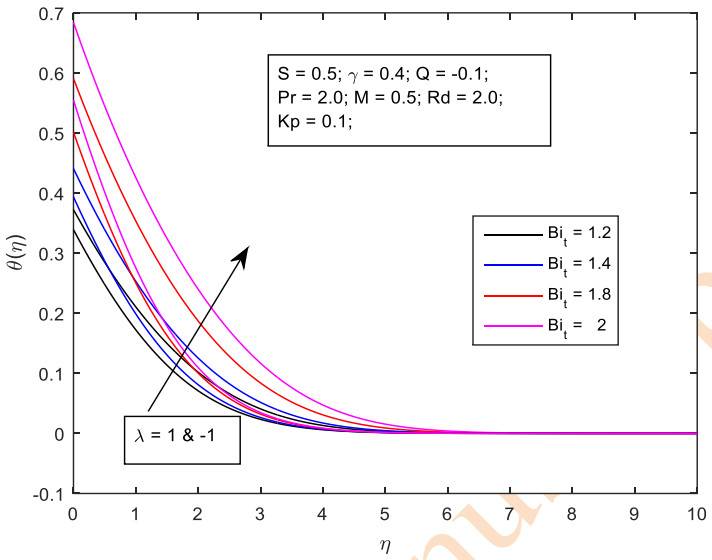

Fig.2(b): Impact of thermal Biot number B_{i_t} on temperature layout $\theta(\eta)$.

The profiles portrayed in Fig. $3(a)$, highlights the repercussion of suction/injection parameter (S) on $f'(\eta)$. We have demonstrated the sequel of S for both aiding flow $(\lambda = 1)$ and contending flow $(\lambda = -1)$ cases. $S > 0$ and $S < 0$ manifests suction & injection orderly and $S = 0$ denote the absence of both. It has been noticed that velocity exhibits opposite nature for aiding and contending flow. In case of aiding flow (demonstrated by solid lines), the negative correlation has been noticed between suction/injection parameter (S) and velocity, but in case of contending flow (represented by dashed lines), the analogous enhancement in value of S exhibits direct relation between suction/injection parameter (S) and velocity layout.

The profiles portrayed in Fig. $3(b)$ depicts the repercussion of S on $\theta(\eta)$. For $\lambda = 1$ and $\lambda = -1$, $\theta(\eta)$ diminishes together with an enhancement in S.

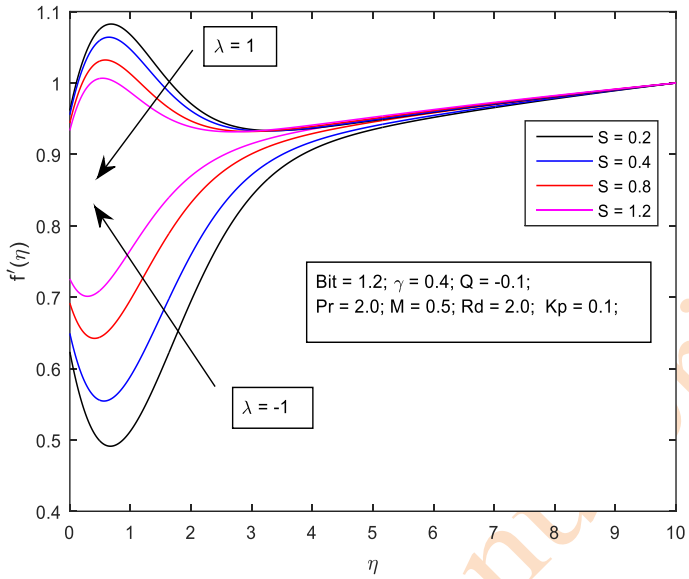

Fig.3(a). Sequel of S on velocity layout $f'(\eta)$.

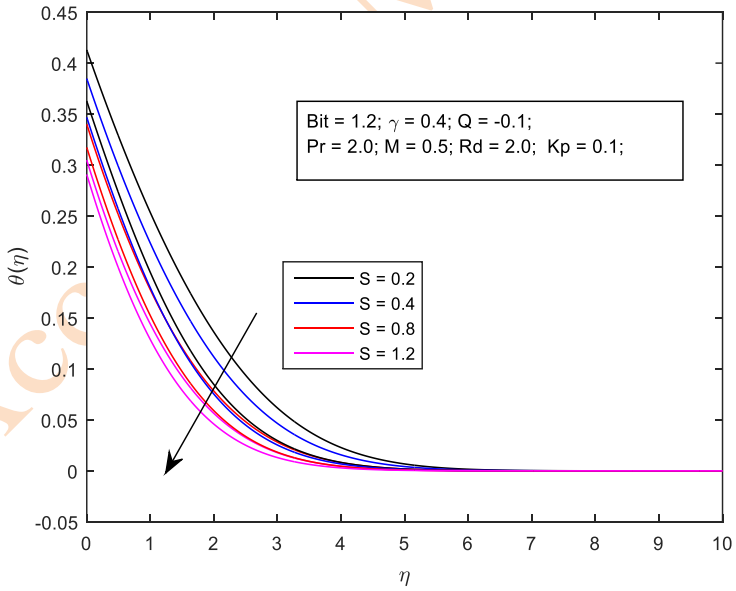

Fig.3(b): Sequel of S on temperature layout $\theta(\eta)$.

The profiles portrayed in Fig.4(a) and 4(b), delineates the impact of heat source/sink parameter (Q) on the velocity layout $f'(\eta)$ and temperature layout $\theta(\eta)$. $Q > 0$

denotes heat generation and $Q < 0$ signifies absorption of heat. We notice the hike in velocity with increment in Q for aiding flow. However, in contending flow, a contrary result has been observed. Numerically positive enhancement of Q connote generation of heat which generating heat in the system consequently uplift the thermal boundary layer thickness of hybrid nanofluid flow. It is found that heat source/sink parameter Q and temperature of hybrid nanofluid flow are positively correlated.

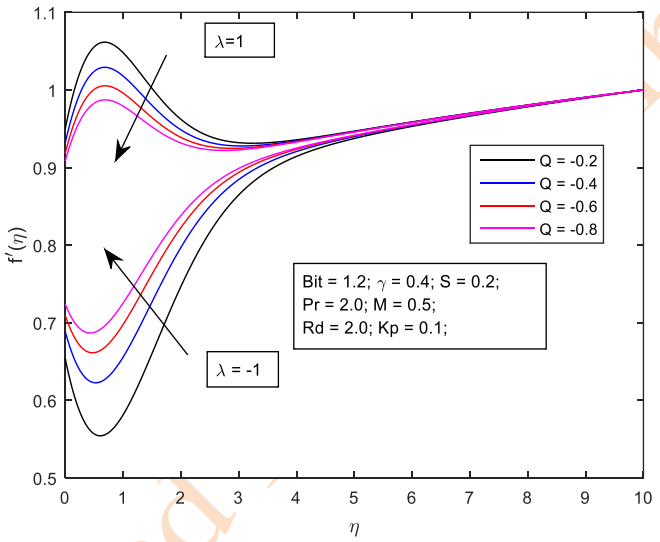

Fig.4(a). Impact of heat source/sink parameter (Q) on $f'(\eta)$.

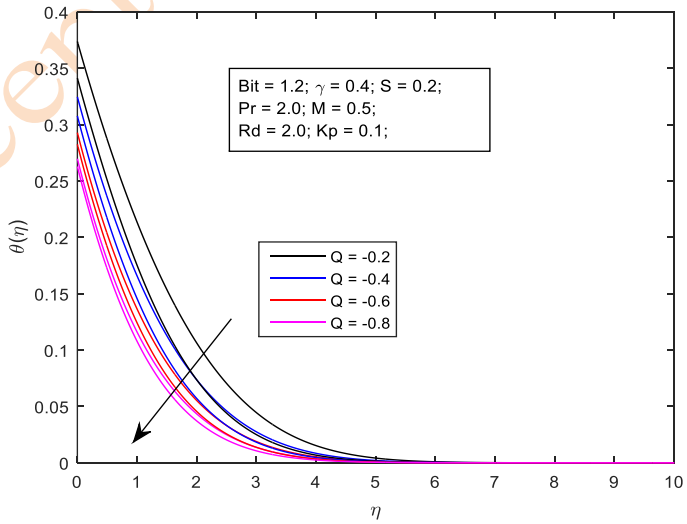

Fig.4(b): Impact of heat source/sink parameter (Q) on $\theta(\eta)$.

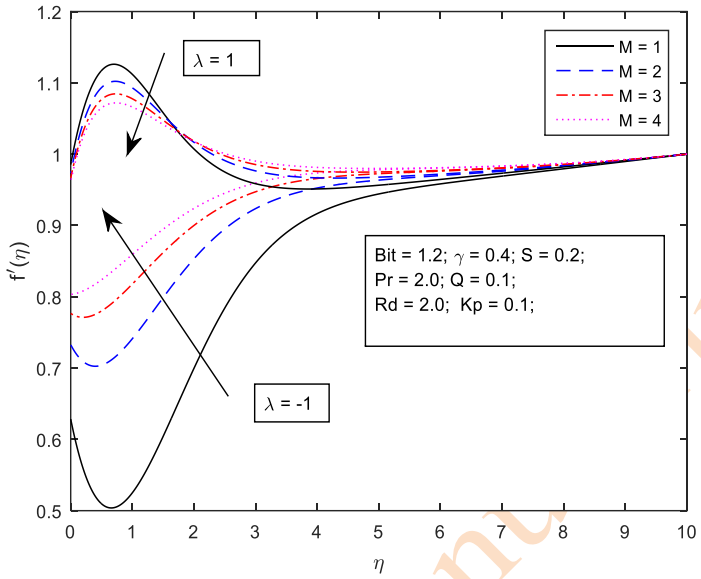

Fig. 5: Impact of magnetic parameter M on $f'(\eta)$.

Fig. 5 displays the alteration in velocity layout $f'(\eta)$ with variant values of M for both aiding flow $(\lambda = 1)$ and contending flow $(\lambda = -1)$ cases. In the region of the stream, positive enhancement in M helps to restore the magnetic field. The enhancement in magnetic parameter M generates the Lorentz force to rise and act against the flow. In both cases $(\lambda = 1\ and\ \lambda = -1)$ velocity layout $f'(\eta)$ increases, when magnetic field parameters M is boosted up.

3. Conclusion

The current research addressed $TiO_2 - MgO/ethylene\ glycol$ based MHD hybrid nanofluid heat transport analysis over a porous media, developing a model to scrutiny the aiding and contending flow. The dominance of leading parameters i.e., suction/injection, heat generation/absorption, and thermal radiative flow have been researched densely and delineated in terms of figures. The impact of velocity slip on boundary layer flow is also analyzed. Moreover, the surface is subjected to convective heating. Some noteworthy outcomes of the present perusal are summarized as follows.

- In comparison to contending flow, for aiding flow the hybrid nanofluid velocity $(TiO_2 - MgO/ethylene\ glycol)$ is found to be lofty.

- Velocity rises with an enhancement of the porosity parameter for aiding flow while for contending flow velocity and porosity parameters are negatively correlated.
- In the case of assisting flow, the thermal Biot number has a direct relation with velocity layout while for the case of opposing flow a contrary result has been observed. $\theta(\eta)$ and thermal Biot numbers are directly related.
- In the case of assisting flow, the slip parameter has a positive correlation with velocity layout while for contending flow a reverse result has been observed.
- In the case of assisting flow, the suction/injection parameter has a negative correlation with velocity layout while for the case of contending flow, a contrary result has been observed. For both i.e., $\lambda = 1$ and $\lambda = -1$, $\theta(\eta)$ and $\varphi(\eta)$ diminish together with an enhancement in $S(suction/injection\ parameter)$.

Acknowledgement: We are thankful to the reviewer and editor for constructive as well as creative suggestions.

References

[1]. Sheikholeslami, M., D. D. Ganji, M. Gorji-Bandpy, and Soleimani S. (2014), Magnetic field effect on nanofluid flow and heat transfer using KKL model, Journal of the Taiwan Institute of Chemical Engineers 45(3), 795-807.

[2]. Sheikholeslami, M., D. D. Ganji, and Rashidi M. M. (2016), Magnetic field effect on unsteady nanofluid flow and heat transfer using Buongiorno model, Journal of Magnetism and Magnetic Materials 416, 164-173**.**

[3]. Heidary, H., Hosseini, R., Pirmohammadi, M., and Kermani, M. J. (2015), Numerical study of magnetic field effect on nano-fluid forced convection in a channel, Journal of Magnetism and Magnetic Materials 374, 11-17**.**

[4]. Imran, M., Umar F., Taseer M., Sami Ullah K., and Hassan W. (2021), Bioconvection transport of Carreau nanofluid with magnetic dipole and nonlinear thermal radiation, Case Studies in Thermal Engineering 26, 101129**.**

[5]. Bagh, A., Sajjad, H., Sohaib A., and Muhammad M.M. (2020), Impact of Stefan blowing on thermal radiation and Cattaneo–Christov characteristics for nanofluid flow containing microorganisms with ablation/accretion of leading edge: FEM approach, The European Physical Journal Plus 135(10), 1-18.

[6]. Ahmad, I., Muhammad F., and Tariq J., (2019), Magneto-nanofluid flow due to bidirectional stretching surface in a porous medium, Special Topics & Reviews in Porous Media: An International Journal 10(5).

[7]. Choi, S. US, and Jeffrey A. Eastman, (1995), Enhancing thermal conductivity of fluids with nanoparticles". Argonne National Lab. (ANL), Argonne, IL (United States).

[8]. Tiwari, R.K., and Manab K. D., (2007), Heat transfer augmentation in a two-sided lid-driven differentially heated square cavity utilizing nanofluids, International Journal of heat and Mass transfer, 50, 9-10.

[9]. Iskandar W., Anuar I., and Ioan P., (2020), MHD flow and heat transfer of a hybrid nanofluid past a permeable stretching/shrinking wedge, Applied Mathematics and Mechanics. 41(3), 507-520.

[10]. Kumar, K.G., Hani, E.H.B., Assad, M.E.H., Rahimi-Gorji, M. and Nadeem, S., (2021). A novel approach for investigation of heat transfer enhancement with ferromagnetic hybrid nanofluid by considering solar radiation". Microsystem Technologies, 27(1), 97-104.

[11]. Shoaib, M., Raja, M.A.Z., Sabir, M.T., Islam, S., Shah, Z., Kumam, P. and Alrabaiah. H., (2020), Numerical investigation for rotating flow of MHD hybrid nanofluid with thermal radiation over a stretching sheet, Scientific Reports, 10 (1), 1-15.

[12]. Chahregh H.S., and Dinarvand. S., (2020), $TiO_2 - Ag/blood$ hybrid nanofluid flow through an artery with applications of drug delivery and blood circulation in the respiratory system, International Journal of Numerical Methods for Heat & Fluid Flow, 30(11), 4775-4796.

[13]. Khan, U., Shafiq, A., Zaib, A., and Baleanu. D., (2020), Hybrid nanofluid on mixed convective radiative flow from an irregular variably thick moving surface with convex and concave effects, Case Studies in Thermal Engineering, 21, 100660.

[14]. Sudarsana R.P., Chamkha. A.J., (2018), Heat and mass transfer characteristics of MHD three – dimensional flow over a stretching sheet filled with water – based Alumina nanofluid, International Journal of Numerical Methods for Heat and Fluid Flow, 28, 532 – 546.

[15]. Yaseen, M., Rawat, S.K., and Kumar. M., (2022), Hybrid nanofluid ($MoS_2 - SiO_2/water$) flow with viscous dissipation and Ohmic heating on an irregular variably thick convex/concave-shaped sheet in a porous medium, Heat Transfer, 51(1), 789-817.

[16]. Iskandar W., Ishak, A. and Pop. I., (2019), Hybrid nanofluid flow and heat transfer past a vertical thin needle with prescribed surface heat flux, International Journal of Numerical Methods for Heat & Fluid Flow, 29(12), 4875-4894.

[17]. Goud, B. S., Kumar, P. P., and Malga. B. S., (2020), Effect of Heat source on an unsteady MHD free convection flow of Casson fluid past a vertical oscillating plate in porous medium using finite element analysis, Partial Differential Equations in Applied Mathematics, 2, 100015.

[18]. Saeed, A., Khan, N.T., Kumam, G.W., Alghamdi, W., and Kumam. P., (2021), The flow of blood-based hybrid nanofluids with couple stresses by the convergent and divergent channel for the applications of drug delivery, Molecules, 26(21), 6330.

[19]. Immanuel, P.N., Chiu, Y.H., and Huang. S.J., (2021), Microfluidic Simulation and Optimization of Blood Coagulation Factors and Anticoagulants in Polymethyl Methacrylate Microchannels, Coatings, 11(11), 1394.

[20]. Yaseen M., Kumar, M., and Rawat. S. K., (2021), Assisting and opposing flow of a MHD hybrid nanofluid flow past a permeable moving surface with heat source/sink and thermal radiation, Partial Differential Equations in Applied Mathematics, 4, 100168**.**

[21]. Abbas, N., Nadeem, S., Saleem, A., Malik, M. Y., Issakhov, A., and Alharbi. F. M., (2021), Models base study of inclined MHD of hybrid nanofluid flow over nonlinear stretching cylinder, Chinese Journal of Physics, 69, 109-117.

[22]. Said, Z., Ghodbane, M., Sundar, L.S., Tiwari, A.K., Sheikholeslami, M., and Boumeddane. B., (2021), Heat transfer, entropy generation, economic and environmental analyses of linear Fresnel reflector using novel $\mathrm{rGO}-\mathrm{Co_3O_4}$ hybrid nanofluids". Renewable Energy, 165, 420-437.

[23]. Huminic G., Huminic. A., (2020), Entropy generation of nanofluid and hybrid nanofluid flow in thermal systems, Journal of Molecular Liquids, 302, 112533.

[24]. Shah, T.R., and Ali. H.M., (2019), Applications of hybrid nanofluids in solar energy, practical limitations and challenges: a critical review, Solar energy, 183, 173 – 203.

[25]. Waini, Ishak, A.and Pop. I., (2019), Unsteady flow and heat transfer past a stretching/shrinking sheet in a hybrid nanofluid, International journal of heat and mass transfer, 136, 288 – 297.